Available online at www.sciencedirect.com

ScienceDirect

Proceedings of the Combustion Institute 000 (2020) 1–8

Proceedings of the Combustion Institute

www.elsevier.com/locate/proci

Evolution and scaling of the peak flame surface density in spherical turbulent premixed flames subjected to decaying isotropic turbulence

Tejas Kulkarni*, Fabrizio Bisetti

Department of Aerospace Engineering and Engineering Mechanics, The University of Texas at Austin, Austin, TX 78712, USA

Received 7 November 2019; accepted 2 June 2020
Available online xxx

Abstract

The peak flame surface density within the turbulent flame brush is central to turbulent premixed combustion models in the flamelet regime. This work investigates the evolution of the peak surface density in spherically expanding turbulent premixed flames with the help of direct numerical simulations at various values of the Reynolds and Karlovitz number. The flames propagate in decaying isotropic turbulence inside a closed vessel. The effects of turbulent transport, transport due to mean velocity gradient, and flame stretch on the peak surface density are identified and characterized with an analysis based on the transport equation for the flame surface density function. The three mechanisms are governed by distinct flow time scales; turbulent transport by the eddy turnover time, mean transport by a time scale related to the pressure rise in the closed chamber, and flame stretch by the Kolmogorov time scale. Appropriate scaling of the terms is proposed and shown to collapse the data despite variations in the dimensionless groups. Overall, the transport terms lead to a reduction in the peak value of the surface density, while flame stretch has the opposite effect. In the present configuration, a small imbalance between the two leads to an exponential decay of the peak surface density in time. The dimensionless decay rate is found to be consistent with the evolution of the wrinkling scale as defined in the Bray-Moss-Libby model.

Keywords: Direct Numerical Simulations; Turbulent spherical flames; Surface density function; Flame wrinkling scale; Bray-Moss-Libby model

1. Introduction

The flamelet regime of turbulent premixed combustion is characterized by an enhancement of the flame surface area, while the local flame structure remains similar to that of a laminar flame. Understanding the mechanisms responsible for the increase of the surface area is critical to the design of combustion devices.

The evolution of the flame surface is often analyzed within the surface density formalism. The flame surface density function (SDF) is defined as

* Corresponding author.
E-mail address: tukulkarni@utexas.edu (T. Kulkarni).

https://doi.org/10.1016/j.proci.2020.06.042
1540-7489

the mean flame surface area per unit volume. The SDF peaks in the middle of the turbulent flame brush and decays rapidly to zero at its edges [1]. The overall burning rate is proportional to the product of the peak surface density and the thickness of the flame brush [2]. While the theory of turbulent diffusion adequately explains the evolution of the flame brush thickness for various configurations [3], at least qualitatively, no such comprehensive theory for the peak surface density exists.

Bray et al. [2] modeled the flame as an infinitesimally thin interface separating the reactants and products. They related the flame surface density function to the flamelet crossing frequency, which is inversely proportional to an integral length scale based on the two-point autocorrelation of the reaction progress variable. This length scale is termed the *wrinkling scale* L^*. Dependence of the ratio L^*/l (where l is the flow integral length scale) on the relative turbulence intensity, u'/S_L has been postulated, but no conclusive evidence exists [4]. Here u' is the velocity fluctuation, and S_L the laminar flame speed.

Alternatively, an evolution equation for the flame surface density may be derived from the *fine grained* PDF formalism [5,6]. The unclosed terms can be modeled to predict the evolution of the surface density. Following this approach, Huh et al. [7] identified the location of the peak surface density and subsequently related the peak value to the statistics of the flame curvature.

In this article, we use an approach inspired by Huh et al. [7] to analyze the evolution of the peak surface density in turbulent premixed flames. We use data from direct numerical simulations of spherical turbulent premixed flames in decaying isotropic turbulence and identify the governing mechanisms affecting the peak value of the surface density function.

Particularly, we seek to address the following questions: How does the peak flame surface density evolve in this configuration? Which quantities control each mechanism? We will relate our findings to the evolution of the wrinkling scale as defined in the Bray-Moss-Libby model [2].

2. Numerical setup

The unsteady reactive Navier–Stokes equations are solved on a Cartesian grid with the massively parallel finite difference solver "NGA" [8] in the low Mach number limit. The spatial discretization for the momentum equation is second order accurate and that for the reactive scalar equations is third order accurate. The time advancement scheme is second order accurate and explicit for the convective terms, while implicit for the diffusive and viscous terms. The variable coefficient pressure Poisson equation is solved instead of the continuity equation using the third party library HYPRE.

Table 1
Simulation parameters. All parameters are at the initial time. Flame scales remain constant in time and across simulations: laminar flame speed $S_L = 1.0$ m/s, thermal thickness $\delta_L = 0.11$ mm, flame time scale $\tau_L = \delta_L/S_L = 0.11$ ms.

	R1K1	R2K1	R3K1	R3K2
N	512^3	1024^3	1024^3	1024^3
Δx (μm)	20	20	20	13.3
u'/S_L	7.4	8.5	9.8	14.7
l/δ_L	3.4	5.2	7.8	4.9
δ_L/η	11.3	11.3	11.5	17.4
R_0/l	3.5	3.4	3.2	3.2
Re_λ	44	59	77	77
Ka	25	25	25	59
Da	0.69	0.91	1.12	0.49
Symbol	◯	□	◇	▽

The system of ordinary differential equations arising from the integration of the chemical sources is advanced in time using CVODE. All simulations are performed in a cubic domain of side L, with periodic boundary conditions in the three directions. Chemical reactions are modeled with a kinetics mechanism featuring a network of 16 species and 73 Arrhenius type reactions, reduced from the GRI 3.0 mechanism [9].

A homogeneous grid with spacing Δx and a constant time step $\Delta t = 0.2$ μs are used. The spatial and temporal resolution of turbulence is ensured with $\eta/\Delta x \geq 0.5$ and $\tau_\eta/\Delta t \geq 20$ for all cases. Here, η and τ_η denote the Kolmogorov length and time scales, respectively. The reactive front is resolved with $\delta_L/\Delta x \approx 5.5$ and $\tau_L/\Delta t \approx 550$, where δ_L and $\tau_L = \delta_L/S_L$ denote the laminar thermal thickness and flame time, respectively. The adequacy of the spatial and temporal resolution of the flame front was previously demonstrated for turbulent premixed jet flames under identical thermo-chemical conditions with extensive numerical tests [10].

A premixed methane/air mixture is considered at equivalence ratio 0.7, initial pressure of 4 atm, and temperature 800 K. Four simulations of spherical flames were conducted by varying the initial turbulence parameters (Table 1). Three simulations, namely R1K1, R2K1 and R3K1, were conducted at different initial Reynolds number $\mathrm{Re}_\lambda = u'\lambda/\nu$, where λ denotes the Taylor micro-scale, u' the velocity fluctuation, and ν the kinematic viscosity of the reactants. The initial Reynolds number varied from 44 to 77, while keeping the initial Karlovitz number $\mathrm{Ka} = \tau_L/\tau_\eta$ constant and equal to 25. Here τ_L denotes the flame time scale. A fourth simulation was conducted at a higher Karlovitz number for the highest Reynolds number (R3K2). The Damköhler number $\mathrm{Da} = \tau/\tau_L$ at the onset is different for all simulations, where $\tau = k/\epsilon$ is the initial eddy turnover time scale. Here k is the turbulent kinetic energy, and ϵ its mean rate of dissipation.

Please cite this article as: T. Kulkarni and F. Bisetti, Evolution and scaling of the peak flame surface density in spherical turbulent premixed flames subjected to decaying isotropic turbulence, Proceedings of the Combustion Institute, https://doi.org/10.1016/j.proci.2020.06.042

The initial velocity field was obtained with auxiliary simulations of homogeneous isotropic turbulence in a smaller domain via the linear forcing scheme. Multiple independent instances were patched together to form a larger domain and discontinuities in the patched state were removed by advancing the fields by $2\tau_\eta$. A spherical kernel of burned gases of radius R_0 was introduced at the origin. The ratio of the kernel radius to integral length scale was kept between $3.2 \leq R_0/l \leq 3.5$ across cases (see Table 1), so that the entire spectrum of turbulent length scales contributes to flame wrinkling at all times.

The simulation was advanced for a time interval over which changes in pressure ($< 20\%$) and temperature ($< 5\%$) are small. This ensures that the laminar flame speed remains constant ($< 1\%$ variation). Similarly, the kinematic viscosity of the reactants changes by less than 10%.

During the outward propagation of the flame, turbulence on the reactants' side decays as in an isothermal decaying isotropic turbulence simulation. The turbulent kinetic energy k decays according to the power law $k/k_0 = (1 + t/t_0)^{-m}$, where k_0, t_0, and m are the initial turbulent kinetic energy, virtual origin, and the decay exponent, respectively. The decay exponent m is 1.55 for all simulations, while the virtual origin t_0 is related to the initial eddy turnover time as $t_0 = m\tau_0$. This value of the exponent is higher than that typically observed in grid generated turbulence [11], but consistent with decaying turbulence simulations at low to moderate Reynolds numbers [12].

The evolution of any turbulence length scale ψ is described by $\psi/\psi_0 = (1 + t/t_0)^\alpha$, indicating that the changes brought by small temporal variations in the kinematic viscosity are inconsequential. The exponent α is 0.64 for the Kolmogorov length scale η, 1/2 for the Taylor micro-scale λ, and 0.225 for $l = u'^3/\epsilon$. We define a transformed logarithmic time scale $s \equiv \log(1 + t/t_0)$ so that $ds = dt/\tau$. All length and time scales of turbulence are exponential functions of s.

3. Results

The propagation of the turbulent spherical flame is described by the reaction progress variable $C(\mathbf{x},\ t)$, defined as $C = 1 - (Y_{O_2} - Y^b_{O_2})/(Y^u_{O_2} - Y^b_{O_2})$. Here Y_{O_2} is the mass fraction of molecular oxygen, and superscripts u and b indicate the values in the reactants and products, respectively. The flame surface is taken to coincide with the isosurface $C = c = 0.73$, the location of maximum heat release rate. The flame surface normal is defined as $\mathbf{n} = -\nabla C/|\nabla C|$ and points towards the reactants. The propagation speed S of the flame surface is given by $S \equiv (|\nabla C|)^{-1}(DC/Dt)$, where D/Dt denotes the Lagrangian derivative.

All relevant statistics depend only on $(r,\ t)$ due to spherically symmetry, which is retained since the flame surface is sufficiently away from the boundaries at all times. The statistics are gathered from a single realization of the flame using spherical averages. During the simulations, the linear extent of the flame R is large compared to the integral scale l by design, so that an adequate number of independent samples are collected. This follows from $R_0/l \approx 3.3$ at $t = 0$ and that the flame radius R grows faster than the integral scale l as turbulence decays.

The propagating flame is described by the probability density function (PDF) of the radial distance of the flame surface from the origin, $\mathcal{P}(r, t)\, dr = dA_r(r, t)/A(t)$, where dA_r is the differential flame surface area within the spherical shell $r \pm dr/2$ and $A(t)$ the total flame surface area at time t.

The PDF is well approximated by a normal distribution $\mathcal{P} = \mathcal{N}(R, \sigma)$, where $\mathcal{N}(R, \sigma)$ denotes the normal distribution with mean R and standard deviation σ. The *flame radius* R is the mean radial distance of the flame surface,

$$R(t) \equiv \mathcal{A}^{-1} \int_{\mathcal{A}} |\mathbf{x}|\, d\mathcal{A}, \tag{1}$$

where $|\mathbf{x}|$ is the Euclidean distance of the surface element $d\mathcal{A}$ from the origin, and the integration is carried out over the flame surface $\mathcal{A}$. Similarly σ is given by

$$\sigma^2(t) \equiv \mathcal{A}^{-1} \int_{\mathcal{A}} (|\mathbf{x}| - R)^2\, d\mathcal{A}, \tag{2}$$

and is termed the *flame brush thickness*. The effects of flame propagation on the temporal variation of R and σ are compensated by defining a *brush coordinate* $\theta = (r - R)/\sigma$. Comparison of $\mathcal{P}(\theta)$ with the model is shown in Fig. 1, and found to be satisfactory.

3.1. Evolution of the peak surface density

The flame surface density function Σ of the flame surface $C = c$ is given by [6]

$$\Sigma = \mathcal{P}_C(C = c)\, \langle\, |\nabla C|\, |\, C = c\, \rangle, \tag{3}$$

where $\mathcal{P}_C$ is the PDF of the reaction progress variable. Here, the angular brackets denote ensemble average, evaluated as averages over spherical shells. The evolution of the flame surface density for spherical flames is described by [6]

$$\frac{\partial \Sigma}{\partial t} + \frac{1}{r^2}\frac{\partial}{\partial r}\left(r^2 \langle\, u_r + S n_r\, \rangle_s \Sigma\right) = \langle\, K\, \rangle_s \Sigma, \tag{4}$$

where u_r and n_r denote the radial projections of the velocity vector $\mathbf{u}$ and the surface normal, respectively. K is the flame stretch rate. Subscript s denotes surface averages, defined as $\langle\, Q\, \rangle_s = \langle\, Q|\nabla C|\, |\, C = c\, \rangle / \langle\, |\nabla C|\, |\, C = c\, \rangle$ for any field Q.

Please cite this article as: T. Kulkarni and F. Bisetti, Evolution and scaling of the peak flame surface density in spherical turbulent premixed flames subjected to decaying isotropic turbulence, Proceedings of the Combustion Institute, https://doi.org/10.1016/j.proci.2020.06.042

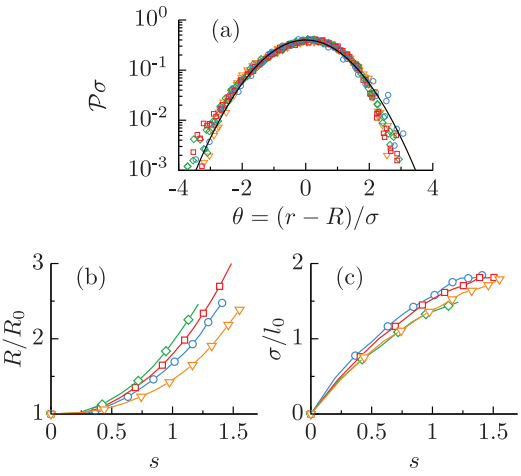

Fig. 1. (a) Normalized PDF of the radial distance versus the brush coordinate. Evolution of (b) the flame radius R and (c) brush thickness σ. Symbols defined as in Table 1.

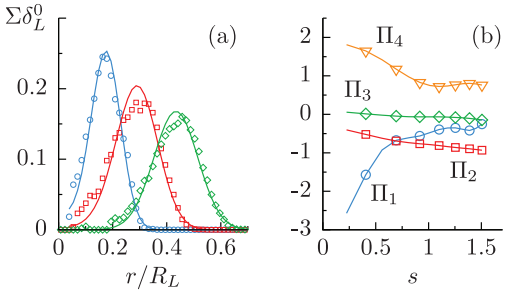

Fig. 2. (a) Comparison of the surface density evaluation with Eq. (3) (symbols), and the model from Eq. (5) (lines). Data shown for flame R2K1 at three instants during its evolution. Time increases from left to right. (b) Terms in the evolution equation, Eq. (8).

An evolution equation for the peak surface density Σ_m may be obtained by evaluating Eq. (4) at the radial distance where $\partial\Sigma/\partial r = 0$. Determination of the radial location of the peak in this manner and using the surface density evaluated with Eq. (3) suffers from statistical noise, so that it is desirable to work with a smooth approximation to Σ based on $\mathcal{P}$. The two are related as $\mathcal{P} = 4\pi r^2\Sigma/A$, since the differential area $dA_r = 4\pi r^2\Sigma dr$. The flame surface density is then modeled as

$$\Sigma = (A/4\pi r^2)\,\mathcal{N}(R,\sigma). \tag{5}$$

Fig. 2a compares Eqs. (5) and (3) and good agreement is seen between the two.

With this model, the location of the peak $\hat{r}(t)$ is

$$\hat{r}/R = 0.5\left[1 + \left(1 - 8\sigma^2/R^2\right)^{1/2}\right]. \tag{6}$$

Since the ratio σ/R is small at all times (Fig. 1c), it follows that $\hat{r} \approx R$. Subsequently, the evolution equation for Σ_m is obtained:

$$\frac{1}{\Sigma_m}\frac{d\Sigma_m}{dt} = \left\{-\frac{1}{r^2}\frac{\partial}{\partial r}(r^2\langle u_r + Sn_r\rangle_s) + \langle K\rangle_s\right\}_{\hat{r}(t)}, \tag{7}$$

where the terms on the right hand side (r.h.s.) are evaluated at $\hat{r}(t)$.

Because the flame radius grows and turbulence decays in time, it is most appropriate to normalize and transform time t and radial distance r as follows: $s = \log(1 + t/t_0), \theta = (r - R(t))/\sigma(t)$. The dimensionless form of Eq. (7) reads

$$\begin{aligned}\frac{d\log\Sigma_m}{ds} = &-\frac{\tau}{\sigma\hat{r}^2}\left\{\frac{\partial}{\partial\theta}(\theta\sigma + R)^2\langle u_r'\rangle_s\right\}_{\hat{\theta}} \\ &-\frac{\tau}{\sigma\hat{r}^2}\left\{\frac{\partial}{\partial\theta}(\theta\sigma + R)^2\langle u_r\rangle\right\}_{\hat{\theta}} \\ &-\frac{\tau}{\sigma\hat{r}^2}\left\{\frac{\partial}{\partial\theta}(\theta\sigma + R)^2\langle Sn_r\rangle_s\right\}_{\hat{\theta}} + \tau\langle K\rangle_s,\end{aligned} \tag{8}$$

where the derivative with respect to θ is to be taken while holding time t constant.

Here, the contributions of the mean velocity field and turbulent fluctuations are separated using the Reynolds decomposition $u_r = \langle u_r\rangle + u_r'$. Note that $\langle u_r'\rangle_s \neq 0$, since $\langle u_r\rangle$ is the *unconditional* mean radial velocity.

The four terms on the r.h.s. of Eq. (8) represent four mechanisms affecting the evolution of the peak flame surface density: turbulent transport (Π_1), mean transport (Π_2), propagation (Π_3), and flame stretch (Π_4). These are shown in Fig. 2b for flame R2K1.

3.2. Transport terms

As seen in Fig. 2b, all transport terms (Π_1, Π_2 and Π_3) contribute to reducing Σ_m. The turbulent transport term (Π_1) dominates early on, but the mean transport term (Π_2) surpasses it later as turbulence decays with time. Propagation (term Π_3) has only a minor influence on the evolution of the peak surface density and its role is primarily to change the peak location $\hat{r}$.

Turbulent transport

Fig. 3a shows the evolution of the magnitude of term Π_1 across simulations. The evolution of this term is identical across different simulations, even though the turbulence intensity is different (see Table 1). To explain this observation, we decompose Π_1 as

$$\Pi_1 = -\frac{\tau}{\sigma}\left\{\frac{2\langle u_r'\rangle_s}{\theta\sigma + R} + \frac{\partial\langle u_r'\rangle_s}{\partial\theta}\right\}_{\hat{\theta}}. \tag{9}$$

Fig. 3b shows the surface averaged radial fluctuation $\langle u_r'\rangle_s$, normalized by the turbulence intensity $u'(t)$ at three instants for each simulation. The self-similarity of the normalized fluctuation $\langle u_r'\rangle_s/u'$

Please cite this article as: T. Kulkarni and F. Bisetti, Evolution and scaling of the peak flame surface density in spherical turbulent premixed flames subjected to decaying isotropic turbulence, Proceedings of the Combustion Institute, https://doi.org/10.1016/j.proci.2020.06.042

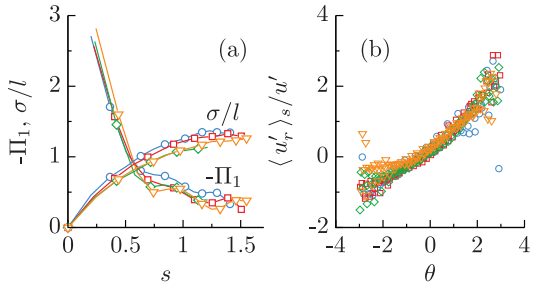

Fig. 3. (a) Absolute value of the term Π_1 and the normalized brush thickness and (b) surface weighted radial fluctuation normalized by reactant side turbulence intensity. Symbols defined as in Table 1.

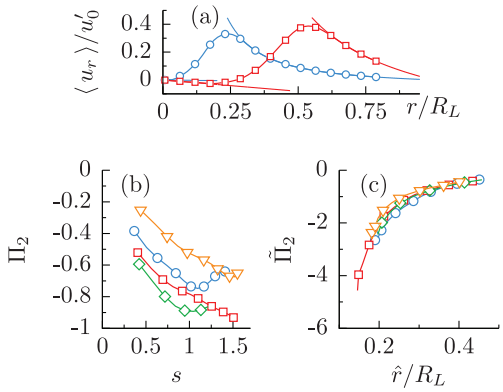

Fig. 4. Mean radial transport of surface density at peak location: (a) mean radial velocity field in the domain (line with symbols), compared to the eqn. (11) (thin lines), (b) term Π_2 of Eq. (8), (c) scaled term $\tilde{\Pi}_2$.

across simulations and in time, along with the observation that $\langle u_r' \rangle_s$ is small at $\hat{\theta}$ (≈ 0), allows for the approximation

$$\Pi_1 \approx -\frac{3}{2}\frac{l}{\sigma}\left\{\frac{\partial \langle u_r' \rangle_s/u'}{\partial \theta}\right\}_{\hat{\theta}}, \tag{10}$$

where we have used the relation $\tau u' = 3u'^3/2\epsilon = 3l/2u'$. The term inside braces is unchanged across simulations, and the first term on the r.h.s. of Eq. (9) is negligible compared to the second term.

The above result shows that the turbulent transport term is inversely proportional to the normalized brush thickness σ/l. Because the evolution of σ/l in the time coordinate s is nearly identical across simulations as shown in Fig. 3a, Π_1 collapses across simulations also.

The scaling of flame brush thickness with the integral scale l is consistent with the literature. The early growth of the flame brush follows Taylor's theory of turbulent diffusion in many turbulent premixed flame configurations [3]. As such, similar scaling of the turbulent transport term Π_1 across different flame configurations is expected, once appropriate modification for the spatial and temporal evolution of turbulence are made. For example, in the present configuration, the early development ($s < 0.5$) of the brush is broadly consistent with the turbulent diffusion theory in decaying turbulence [13]. Differences appear across simulations later ($s > 1.2$) due to several additional effects such as the gradient of the mean radial velocity [14] and differential flame stretch effects, wherein surface is produced mainly at the leading edge and destroyed at the trailing edge. Nevertheless, these differences are small and are ignored in the context of the term Π_1.

Mean transport

The propagation of the reactive front induces a mean radial velocity due to thermal expansion across the flame. The gradient of the mean radial velocity in turn affects the peak surface density through the term Π_2. An analytical expression for the mean radial velocity outside the turbulent brush is readily obtained by solving the Reynolds averaged continuity equation, assuming uniform density in reactants and products. The density changes isentropically in time with pressure. A general solution for the mean radial velocity field is $\langle u_r \rangle = -(r/3\gamma p)\, dp/dt + C_u r^{-2}$, where C_u is a constant and γ is the specific heat ratio.

On the products' side, $\langle u_r \rangle = 0$ at $r = 0$ implies $C_u = 0$. The distance to the boundary in the reactants depends on the azimuthal and polar angles. However, the mean radial velocity in the reactants decreases as r^{-2} and the field can be assumed symmetric when the flame surface is far from the boundaries. By imposing the zero velocity boundary condition at an *effective domain radius* $R_L \equiv L(3/4\pi)^{1/3} \approx 0.62L$, the mean radial velocity in the reactant and product sides is given by

$$\langle u_r \rangle(r,t) = \begin{cases} -\dfrac{R_L}{3\gamma_p p}\dfrac{dp}{dt}\left(\dfrac{r}{R_L}\right) & \text{Products} \\ -\dfrac{R_L}{3\gamma_r p}\dfrac{dp}{dt}\left[\dfrac{r}{R_L} - \left(\dfrac{r}{R_L}\right)^{-2}\right] & \text{Reactants} \end{cases} \tag{11}$$

In the above expression, γ_p and γ_r are the specific heat ratios of the products and reactants, respectively. Fig. 4a shows that the mean radial velocity is well approximated by Eq. (11) outside the brush.

The previous analysis does not model the mean velocity field within the brush, but highlights the relevant quantities that control Π_2. The expression for Π_2 reads

$$\Pi_2 = -\frac{\tau}{\sigma \hat{r}^2}\left\{\frac{\partial}{\partial \theta}(\theta\sigma + R)^2 \langle u_r \rangle\right\}_{\hat{\theta}}. \tag{12}$$

The factor of R_L/τ_p, where $\tau_p \equiv p(dp/dt)^{-1}$ appears in front of radial velocity in both reactants

Please cite this article as: T. Kulkarni and F. Bisetti, Evolution and scaling of the peak flame surface density in spherical turbulent premixed flames subjected to decaying isotropic turbulence, Proceedings of the Combustion Institute, https://doi.org/10.1016/j.proci.2020.06.042

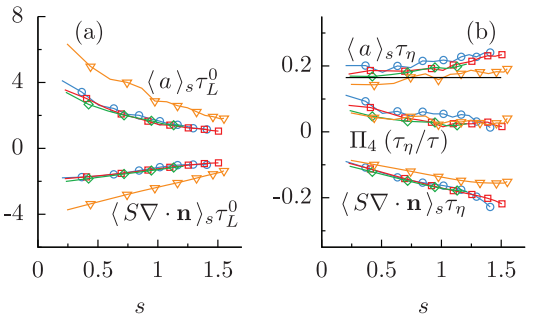

Fig. 5. Flame stretch and components (a) normalized by flame time $\langle K \rangle_s \tau_L$ and (b) by the instantaneous Kolmogorov time scale $\langle K \rangle_s \tau_\eta$. Solid line marks $a\tau_\eta = 0.165$ found for infinitesimal elements in isothermal turbulence [15]. Symbols as defined in Table 1.

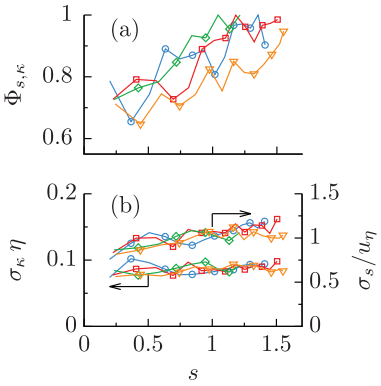

Fig. 6. (a) Correlation coefficient $\Phi_{s,\kappa}$ and (b) Scaling of standard deviations of s and κ with the respective Kolmogorov scales. Symbols as defined in Table 1.

and products and can be expected to affect Π_2 as well. The re-scaled term $\tilde{\Pi}_2 \equiv \Pi_2\,(\tau_p/\tau)\,(\sigma/R_L)$ is shown to collapse across simulations in Fig. 4c. Similarity of $\tilde{\Pi}_2$ across simulations indicates that the mean transport term depends on the ratio of the flame brush thickness to the effective domain radius (σ/R_L) and the ratio of the pressure rise time scale to the eddy turnover time (τ_p/τ).

3.3. Flame stretch

Flame stretch acts as a source of surface density and contributes to increasing its peak. Stretch consists of two terms [5] $\Pi_4 = \langle K \rangle_s \tau = \langle a \rangle_s \tau + \langle S\nabla \cdot \mathbf{n} \rangle_s \tau$. The tangential strain rate $a \equiv -\mathbf{nn} : \nabla \mathbf{u} + \nabla \cdot \mathbf{u}$ describes the effect of turbulent straining, while the second term describes the effect of propagation in the presence of curvature. The two terms are shown in Fig. 5a for all simulations, normalized by the flame time scale. The flame stretch is positive overall and small in magnitude compared to its two contributions. The magnitude of both terms decreases in time.

It has been shown that the tangential strain rate for infinitesimal material surface in homogeneous isotropic turbulence is governed by the Kolmogorov time scale. Girimaji and Pope [15] concluded that $a\tau_\eta$ is independent of Reynolds number in the range $\mathrm{Re}_\lambda = 38 - 90$. This behavior was attributed to the alignment of the surface normal along the direction of the eigenvector corresponding to the most compressive eigenvalue of the velocity gradient tensor [15,16], which leads to persistent straining of the surface.

Fig. 5b shows the two terms and flame stretch normalized by τ_η, evaluated in the reactants. The turbulence statistics at the flame surface $C = c$ evolve similarly to that in the reactants to within a constant (not shown). As with infinitesimal material surfaces, we observe $\langle a \rangle_s \tau_\eta \approx 0.2$, independent of Reynolds number. Once normalized by τ_η, the tangential strain rate term is constant in time to within 20%, compared to a twofold change in $a\tau_L$. The origin of the residual temporal dependence is unclear at the moment and may be related to some large scale effects specific to this flame configuration. It appears that this slow evolution is slightly different across simulations and smaller for larger Reynolds numbers.

The normalized curvature term is given by

$$\langle S\nabla \cdot n \rangle_s \tau = \langle -2S\kappa \rangle_s \tau = \tau \frac{\langle S\kappa |\nabla C| \,|\, C = c \rangle}{\langle |\nabla C| \,|\, C = c \rangle} \tag{13}$$

and shows a much larger temporal variation, although the temporal evolution across simulations is similar. This term is mainly controlled by fluctuations in the curvature and the displacement speed, since the flame surface is mostly flat in the middle of the brush, and $\langle \kappa \rangle_s \approx 0$ at peak location $\hat{r}(t)$.

To analyze the fluctuation term, we define a gradient weighted flame speed $\tilde{S}(r,t) = S|\nabla C|/\langle |\nabla C| \,|\, C = c \rangle$ and its corresponding fluctuation S'. The decomposition $S \equiv \tilde{S} + S'$ in Eq. (13) leads to the expression: $-2\langle S\kappa \rangle_s = -2\langle S'\kappa \rangle_s = -2\Phi_{s,\kappa}\sigma_s\sigma_\kappa$. Here $\Phi_{s,\kappa}$ is the correlation coefficient between $\tilde{S}$ and κ, and σ_s and σ_k are the corresponding standard deviations.

The correlation coefficient $\Phi_{s,\kappa}$ is nearly unity, and changes by about 30% in time (Fig. 6a). On the other hand, the normalized quantities σ_s/u_η and $\sigma_\kappa \eta$ are roughly constant in time and across simulations as shown in Fig. 6b. Specifically, the collapse across R3K1 and R3K2 is convincing where η and u_η differ by a factor of 1.5.

It is clear from the above analysis that the flame stretch is governed by τ_η for the most part and that the product $\langle K \rangle_s \tau_\eta$ changes in time due to changes in the correlation coefficient $\Phi_{s,\kappa}$. The reasons behind this behavior are not clear at present and war-

Please cite this article as: T. Kulkarni and F. Bisetti, Evolution and scaling of the peak flame surface density in spherical turbulent premixed flames subjected to decaying isotropic turbulence, Proceedings of the Combustion Institute, https://doi.org/10.1016/j.proci.2020.06.042

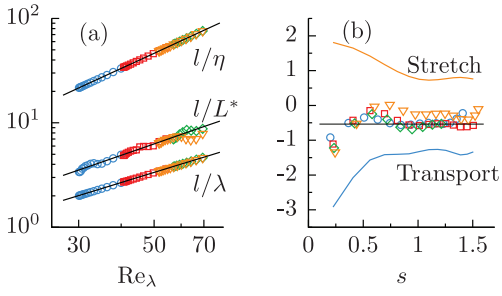

Fig. 7. (a) Length scale ratios l/η, l/λ and l/L^* versus Taylor Reynolds number. (b) Balance of all terms that control the evolution of Σ_m. Stretch (Π_4) and transport ($\Pi_1 + \Pi_2 + \Pi_3$) terms (lines) are shown for R2K1. The sum of all four terms is also shown (symbols) for all simulations, and thin line marks $\alpha_\Sigma = -0.5357$ according to Eq. (14). Symbols as defined in Table 1.

rant further investigation, over a broader range of the dimensionless parameters. As a consequence of the above analysis, the flame stretch term may be modeled as $\Pi_4 = f(s)\,(\tau/\tau_\eta) = C_\eta f(s)\,\mathrm{Re}_\lambda$, where the function $f(s)$ captures the temporal dependence of $\Phi_{s,\kappa}$ and C_η is the proportionality constant between τ/τ_η and Re_λ.

3.4. Evolution of the peak surface density

The logarithmic time rate of change $d\log\Sigma_m/ds$ depends on the balance of transport (sum of Π_1, Π_2 and Π_3) and stretch (Π_4) in Eq. (8). While the mean velocity term (Π_2) is configuration specific, some universality in the scaling of the turbulent transport (Π_1) and the differential stretch (Π_4) terms is expected. This postulate is supported by the observation that the evolution of the flame brush thickness is broadly consistent with the turbulent diffusion theory, while the flame stretch term scales with the instantaneous Kolmogorov time scale, as for material surface elements in isotropic turbulence [15]. In the present flame configuration, we observe that a small imbalance between the transport and the stretch terms results in Σ_m decreasing with time.

Fig. 7 (a) shows the evolution of the peak surface density, represented as the ratio l/L^*. Here, we take the wrinkling scale as $L^* \equiv (4\Sigma_m)^{-1}$, consistent with the Bray-Moss-Libby (BML) model [2]. The length scale ratios l/λ and l/η are also shown for comparison. A least squares power law fit for the ratio l/L^* gives $l/L^* = 0.0756\,\mathrm{Re}_\lambda^{1.13}$.

Within this model, $d\log\Sigma_m/ds$ is a constant, given by

$$\alpha_\Sigma \equiv \frac{d\log\Sigma_m}{ds} = \frac{d\log(\mathrm{Re}_\lambda^{1.13} l^{-1})}{ds} = -0.5357 \tag{14}$$

Fig. 7(b) compares data from simulations with the constant α_Σ. Apart from an initial transient, the rate of change $d\log\Sigma_m/ds$ is consistent with the model. The logarithmic rate of change α_Σ is constant even as the terms Π_1, Π_2 and Π_4 show significant temporal variations. The higher Karlovitz flame R3K2 features a smaller (in magnitude) rate of decay, reasons for which are unclear at this point. Such behavior may be due to a dependence on the Karlovitz number, Damköhler number, or other dimensionless groups that were not kept constant.

The Reynolds number dependence of the ratio l/L^* may be in part due to that of the stretch term Π_4. The flame stretch is governed at the dissipative scales, while the transport of surface density occurs on larger time scales (turbulent transport on eddy turnover scale τ and mean transport on pressure rise scale τ_p). The evolution of the peak surface density appears to be affected by the separation of these scales, as parameterized by Re_λ. The proposed power law fit is based on simulations of spherical flames in decaying isotropic turbulence and may not be universal. Furthermore, the trends observed here should be assessed at higher values of the Reynolds number when all scales are more separated and the inertial range is broader.

4. Conclusions

In this work, we examined the evolution of the peak flame surface density in spherical turbulent premixed flames subjected to freely decaying isotropic turbulence in a closed vessel. The evolution of Σ_m follows an exponential decay in the transformed logarithmic time s, consistent with a power law for the wrinkling scale $L^* = (4\Sigma_m)^{-1}$ given by $l/L^* \sim \mathrm{Re}_\lambda^{1.13}$ proposed recently by the authors [17]. The mechanisms affecting the evolution of the peak surface density were identified and investigated. The evolution of Σ_m is controlled by a small imbalance between three mechanisms, i.e. turbulent transport, mean transport, and flame stretch. A Reynolds number dependence of the Bray-Moss-Libby wrinkling scale is related to the ratio of the eddy turnover time and the Kolmogorov time as it appears in the ordinary differential equation governing the evolution of Σ_m.

Declaration of Competing Interest

No conflict of interest.

Acknowledgments

Tejas Kulkarni and Fabrizio Bisetti are sponsored in part by NSF grant #1805921. Numerical simulations were carried out on the "Shaheen" supercomputer at King Abdullah University of Science and Technology (KAUST); and on

Please cite this article as: T. Kulkarni and F. Bisetti, Evolution and scaling of the peak flame surface density in spherical turbulent premixed flames subjected to decaying isotropic turbulence, Proceedings of the Combustion Institute, https://doi.org/10.1016/j.proci.2020.06.042

the "Stampede2" supercomputer at the Texas Advanced Computing Center (TACC) through the allocation TG-CTS180002 under the Extreme Science and Engineering Discovery Environment.

References

[1] J. Hult, S. Gashi, N. Chakraborty, M. Klein, K.W. Jenkins, S. Cant, C.F. Kaminski, *Proc. Combust. Inst.* 31 (1) (2007) 1319–1326.
[2] K.N.C. Bray, M. Champion, P.A. Libby, *Symp. (Int.) Combust.* 22 (1) (1989) 763–769.
[3] A. Lipatnikov, *Fundamentals of Premixed Turbulent Combustion*, CRC Press, 2012.
[4] B. Renou, A. Mura, E. Samson, A. Boukhalfa, *Combust. Sci. Technol.* 174 (4) (2002) 143–179.
[5] S.B. Pope, *Int. J. Eng. Sci.* 26 (5) (1988) 445–469.
[6] L. Vervisch, E. Bidaux, K. Bray, W. Kollmann, *Phys. Fluids* 7 (10) (1995) 24962503.
[7] K.Y. Huh, J. Kwon, D. Lee, *Phys. Fluids* 25 (7) (2013) 075108.
[8] O. Desjardins, G. Blanquart, G. Balarac, H. Pitsch, *J. Comput. Phys.* 227 (15) (2008) 71257159.
[9] S. Luca, A.N. Al-Khateeb, A. Attili, F. Bisetti, *J. Propul. Power* 34 (2018) 153–160.
[10] S. Luca, A. Attili, E.L. Schiavo, F. Creta, F. Bisetti, *Proc. Combust. Inst.* 37 (2) (2019) 2451–2459.
[11] P.-A. Krogstad, P.A. Davidson, *J. Fluid Mech.* 642 (2010) 373394.
[12] P. Burattini, P. Lavoie, A. Agrawal, L. Djenidi, R.A. Antonia, *Phys. Rev. E* 73 (2006) 066304.
[13] M. Huang, A. Leonard, *Phys. Fluids* 7 (10) (1995) 2455–2464.
[14] I. Ahmed, N. Swaminathan, *Combust. Sci. Technol.* 185 (10) (2013) 1509–1540.
[15] S.S. Girimaji, S.B. Pope, *J. Fluid Mech.* 220 (1990) 427458.
[16] A. Tsinober, *An Informal Conceptual Introduction to Turbulence*, 483, Springer, 2009.
[17] T. Kulkarni, R. Buttay, M.H. Kasbaoui, A. Attili, F. Bisetti, *J. Fluid Mech.* (2020). Under review.

Please cite this article as: T. Kulkarni and F. Bisetti, Evolution and scaling of the peak flame surface density in spherical turbulent premixed flames subjected to decaying isotropic turbulence, Proceedings of the Combustion Institute, https://doi.org/10.1016/j.proci.2020.06.042